



PHYSICAL FOUNDATIONS DETERMINING SPECTRAL CHARACTERISTICS MEASURED IN BRAGG GRATINGS SUBJECTED TO BENDING

Piotr Kisała

Lublin University of Technology, Nadbystrzycka 38A, 20-618 Lublin, Poland (✉ p.kisala@pollub.pl, +48 81 538 42 99)

Abstract

The article presents an analysis of the impact of bending optical fibers with tilted Bragg gratings on their spectral parameters. This article proves that it is possible to choose TFBG cladding mode and the optical spectrum range related to it that allows the best metrological properties to be obtained when measuring bend. The results contained in the paper explain why the minima in the spectral characteristics, corresponding only to some cladding modes, change their shape during TFBG bending, which is important for application of Bragg gratings as bending sensors. It has been presented that in the case of TFBG we are able to aggregate the knowledge obtained during experiment to the form of a physical model of the fiber bending sensor.

Keywords: optical fibers, tilted fiber Bragg grating, bending sensors.

© 2022 Polish Academy of Sciences. All rights reserved

1. Introduction

For years, the analysis of physical phenomena taking place in optical systems has created many new development paths and the possibility of using them as optical or optoelectronic sensors [1, 2]. Optical methods of measuring physical quantities have been widely researched and developed [3]. Ordinary fiber Bragg gratings (FBG) and their numerous variations, *e.g.*, in the form of oblique structures, are increasingly used as converters of mechanical quantities into optical parameters [4–6]. The use of these elements as bending sensors requires, for example, their placement in photonic fibers with photonic gap PBGFs (all-solid photonic bandgap fibers) [7]. However, such a solution is very sensitive to the effects of inaccuracies in the geometry of microstructural fibers. Bending measurement systems using LPFGs, FBGs [8] and TFBGs [9, 10] are also tested. Reduction of cross-sensitivity to temperature of this type of structure is often carried out by using hybrid structures, also composed of two types of optical gratings: LPFG and TFBG. In this way, changes in the bending radius can be investigated [11]. Some of the sensors using TFBG elements can also be considered temperature independent [12] by inserting a segment of a multimode fiber between the single mode fiber and the TFBG element. Structures used as bending sensors are also known [13], in which the FBG grating is written in the same place as

the TFBG (superimposed grating structure). In such systems, the signal reflected from the FBG grating is modulated by a TFBG, which is sensitive to bending [14]. Among the existing methods of measuring bends by using TFBG elements, it is necessary to mention those that allow the measurement of macro bends with very small values [15]. For example, in [16], a very promising method was proposed, but it only allows for the measurement of the bend radius. Additionally, in the assumptions of this method, it is possible to measure only a few discrete bend values. When analyzing the existing solutions of TFBG-based sensors for bending measurement, the aim is to develop solutions that will be insensitive to temperature changes, although the measuring transducer is an optical fiber with a Bragg grating [17]. A desirable feature is also the ability to measure other physical quantities with the same measuring element. In the works on the use of TFBG elements as bending transducers of the optical fiber for changes in optical parameters of propagating light, there is neither analysis of individual spectral ranges nor a comparison of the behavior of individual propagating modes in the optical fiber subject to bending. Additionally, there is no direct analysis explaining for which angles and modes of the TFBG structure it is possible to obtain the maximization of its sensitivity to bending.

The physical rule determining the properties of spectral characteristics observed for Bragg gratings subjected to bending is indeed known, but in the case of tilted Bragg structures, the spectral evolution of individual modes is not sufficiently explained. The motivation to research this topic was also the lack of studies showing the possibility of optimizing the physical parameters of TFBG used as a bend sensor.

Therefore, this paper reports on the conditions under which it is possible to achieve the greatest spectral shifts. The angles of the TFBG structures were determined, and specific linearly polarized (LP) modes were indicated for which such a maximization of shifts is possible. The conditions under which the measurement range is significantly limited and the spectral characteristics of the examined structures are distorted were also indicated, preventing their use as sensors of physical quantities. Modes whose measurement of spectral shifts is the most favorable from the point of view of maximizing the sensitivity to bending have also been indicated.

2. Spectral shift for selected modes measured with the TFBG structure

Changes in the shift of individual modes depend on the direction of application of the bending force, so it is necessary to determine it precisely. This paper presents the results of spectral measurements for the case where the force acts parallel to the x -axis of the optical fiber coordinate system with written tilted diffraction patterns forming the TFBG structure (Fig. 1).

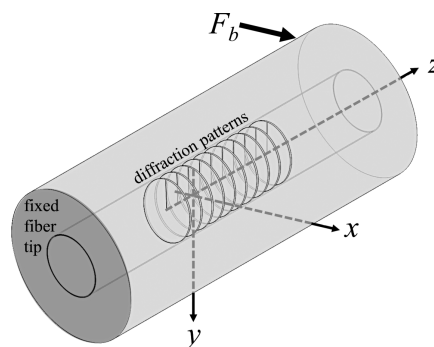


Fig. 1. Geometry of the TFBG measurement system during fiber bending.

The structure was recorded on an optical fiber (Corning SMF-28) with the single-mode phase mask method using ultraviolet radiation at a wavelength of 248 nm. The system for producing Bragg structures was modified in such a way as to obtain the slope of the diffraction patterns equal to 2° . The total length of the structure was 15 mm, and Bragg resonance occurred at a wavelength of 1564.5 nm.

Controlled bending was applied at a stable temperature (22°C) during recording of the TFBG in the optical fiber. Spectral measurements were made in the transmission system of the fibers prepared in this way with TFBG structures, according to the diagram shown in Fig. 2.

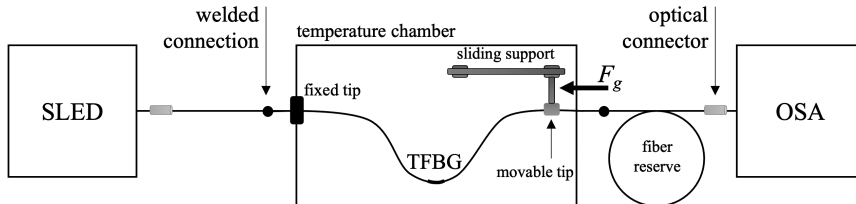


Fig. 2. Scheme of the measurement system.

The characteristics of the TFBG structure produced with an excimer laser and measured in the measuring system shown in Fig. 2 are shown in Fig. 3. Measurements were made for neutral conditions (unbent fiber; bending force $F_g = 0$) and for bending with radius $R = \infty$.

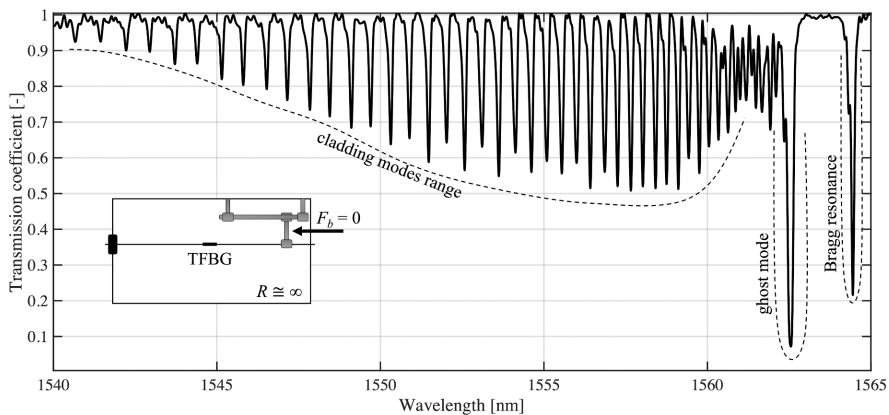


Fig. 3. Spectral characteristic of the produced TFBG measured in the transmission system in the absence of a bending force.

Figure 3 shows three areas of the spectrum that were further considered, *i.e.*, the area of the minima related to the existence of cladding modes in the structure, the minimum related to the ghost mode and the Bragg resonance area. Figure 4 shows the situation in which the optical fiber with the TFBG structure written down was bent due to the nonzero bending force $F_g \neq 0$.

Some of the minima on the transmission characteristics corresponding to the cladding modes have been significantly shifted. The height of these minima has also changed. This means that the transmission coefficient for a given minimum derived from the cladding mode also changes. A more detailed analysis of these changes is presented in the next chapter.

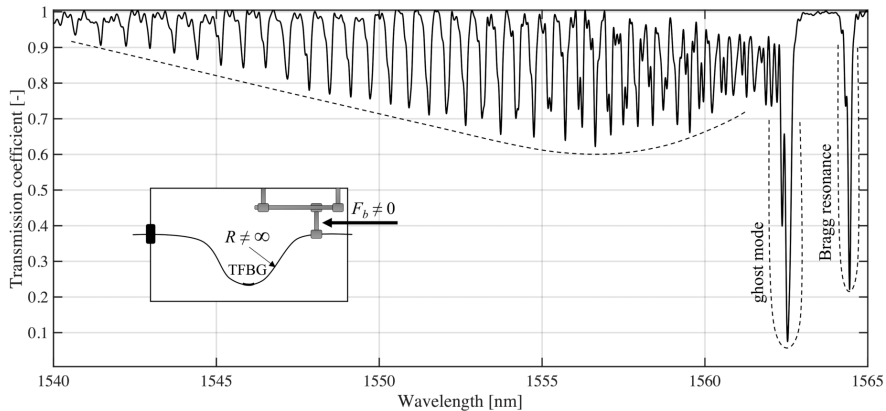


Fig. 4. Spectral characteristics of a bent TFBRG measured in the transmission mode.

3. Analysis of changes in spectral characteristics of TFBRGs subjected to bending

3.1. Spectral shifts in TFBRG fibers

Figures 3 and 4 are only illustrative, and the exact values of the bending radii and their influence on the spectral responses of the manufactured TFBRG transmitters are presented later in the paper. Fig. 5 shows the changes in Bragg resonance (Fig. 5a), ghost mode (Fig. 5b) and the two selected linearly polarized modes most responsive to changes in the bend radius of the fiber, *i.e.*, LP₁₁₀ (Fig. 5c) and LP₀₁₅ (Fig. 5d).

The characteristics presented in Fig. 5 have been measured for bending radii varying from 30 mm to 15 mm. The optical fiber shows a bending loss below the critical bending radius. For SMF-28 at a wavelength of 1.5 μm , the critical bending radius is 6–8 mm [18]. Therefore, in this paper, a safe range of bending radii from 30 to 15 mm was selected. The gray dotted line marks the waveforms measured with a bend radius of 30 mm, while the dashed black line marks the characteristics measured with a bend radius of 15 mm. The selected TFBRG modes react with different sensitivities to changes in the bend radius of the fiber. When analyzing the entire spectral characteristics, two modes can be distinguished: LP₁₁₀ (Fig. 5c) and LP₀₁₅ (Fig. 5d), for which the spectral shift caused by the change in the bending radius by 15 mm is the greatest. To visualize the spectral shift for the selected 4 modes, *i.e.*, Bragg resonance (Fig. 5a), ghost mode (Fig. 5b), LP₁₁₀ (Fig. 5c) mode and LP₀₁₅ (Fig. 5d) mode, transmission characteristics were measured for fibers bent from 30 mm to 15 mm in 0.5 mm steps at constant, controlled temperature. The results of these measurements are summarized in Fig. 6, which shows the processing characteristics of the TFBRG bend sensor.

Both the minimum associated with the Bragg resonance (Fig. 6a) and the lower-order modes that make up the ghost mode (Fig. 6b) are subjected to a practically negligible spectral shift. The wavelength change for these minima is 10 pm. The situation is different in the case of the LP₁₁₀ and LP₀₁₅ modes. In the case of the LP₁₁₀ mode, the change in the minimum wavelength associated with its existence in the transmission characteristics of the fiber with the TFBRG is approx. 280 pm (Fig. 6c), while for the LP₀₁₅ mode, it is 170 pm (Fig. 6d). It is also worth noting that in the case of the LP₀₁₅ mode, the processing characteristic is monotonic over the entire range of changes in the bend radius from 30 mm to 15 mm. In the case of the LP₁₁₀ mode, several

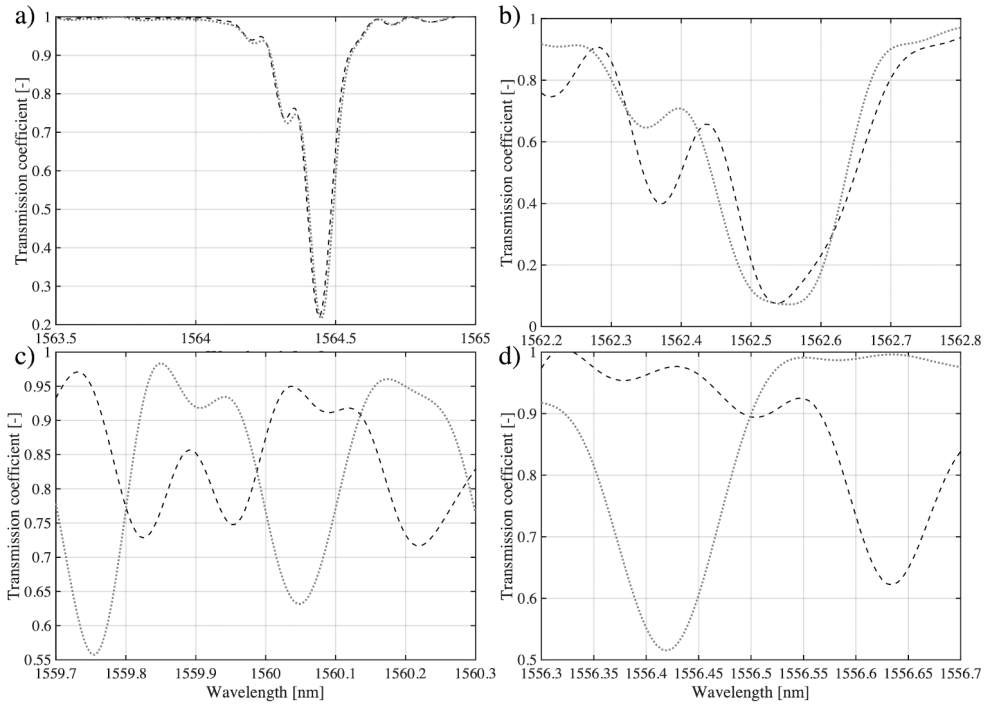


Fig. 5. Modifications of individual modes of the TFBG structure subjected to bending, Bragg resonance (a), ghost mode (b), LP₁₁₀ (c), and LP₀₁₅ (d).

areas of changes in the wavelength shift as a function of the change in the bending radius can be distinguished. The monotonic decrease in the value of the spectral shift in the case of this mode occurs from 15.5 nm, and this decrease is nonuniform for the entire range of bend radius changes and is the largest for bend radii of approximately 17 mm and 22 mm. The reaction of individual cladding modes to bending can be expressed by defining the sensitivities of the spectral shift of a given mode per bending unit. In the case under consideration, it will be most convenient to take the size of the bend radius as a measure of the bending since it takes the same value along the entire length of the TFBG structure. The expression specifying the bending sensitivity defined in this way will be written in the following form:

$$S_{LP_{min}} = \frac{\Delta\lambda_{min}}{\Delta R}, \quad (1)$$

where $\Delta\lambda_{min}$ is the change in the minimum wavelength of the selected mode, ΔR is the change in the bend radius length causing the spectral shift of the mode, m is the azimuth number of the mode, $m = 0$ or 1 , and n is the radial number of the mode. The spectral shift caused by the reduction of the fiber bend radius for the LP₁₁₀ mode is 18.7 pm/mm. Mode LP₁₁₀ moves within the considered range of the bending radius by 0.28 mm (Fig. 6). In turn, in the case of the LP₀₁₅ mode, the spectral shift is only 0.17 nm, which gives a sensitivity of 11.3 pm/mm. Thus, the spectral shift can be a measure of the flexure of the fiber with the TFBG, and it is important to know the mode number whose shift is measured. The explanation of the differences in shifts of individual cladding modes due to bending has been included in a further part of the work.

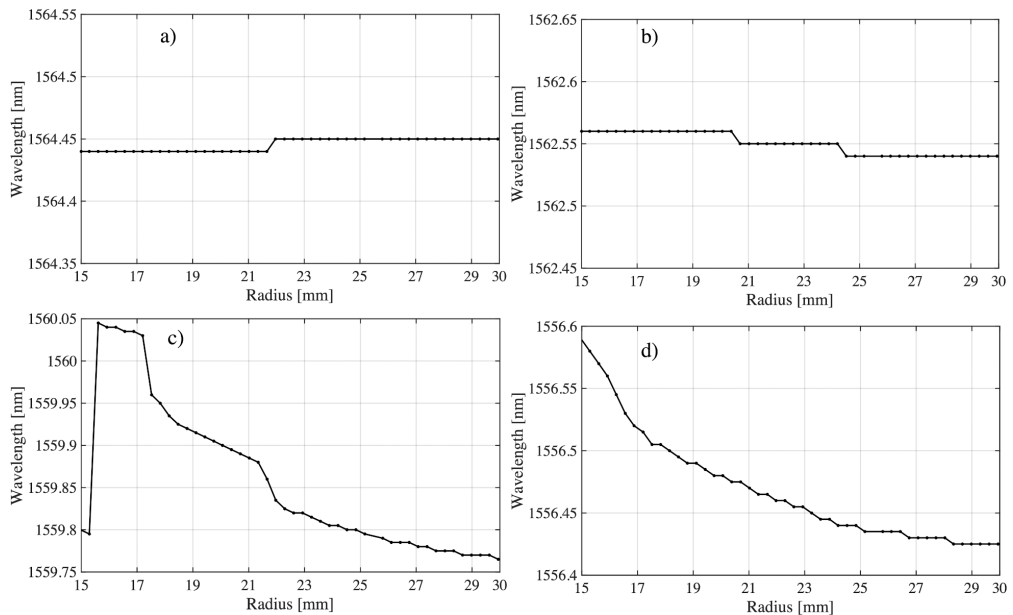


Fig. 6. Characteristics of TFBBG processing when subjected to bending for selected propagating modes in the structure: Bragg resonance (a), ghost mode (b), LP₁₁₀ (c), and LP₀₁₅ (d).

Other modes also undergo a spectral shift. The LP₀₁₆ mode also shifts with a sensitivity factor $S_{LP_{016}}$ of 8.4 pm/mm. Successive higher-order modes are also shifted due to the bending of the entire structure. For example, LP₀₁₇ is shifted by 6.8 pm for each millimeter of change in the structure's bending radius. In the considered range of bending changes, the total shift of the LP₀₁₇ mode is 130 μ m. It is also characteristic that in the TFBBG structure, all modes of order higher than LP₀₁₇ have ever-lower values of the bending shift sensitivity coefficient. For example, the LP₀₁₈ mode only shifts by 105 μ m. The bending sensitivity factor for this mode is only $S_{LP_{018}} = 7$ pm/mm. The spectral shift of the LP₁₁₉ mode is now only 45 pm. The $S_{LP_{119}}$ coefficient of this mode is 3 pm/mm, while the wavelengths of the LP₁₂₂ mode change only by 25 pm, which in turn corresponds to the $S_{LP_{119}}$ sensitivity of this mode at only 1.7 pm/mm. It is characteristic that for a TFBBG with a tilt angle of the diffraction planes amounting to 2°, for all the higher order cladding modes, with azimuth numbers of 0 and 1, starting from LP₀₂₄, the spectral shift phenomenon is practically negligible, *e.g.*, for LP₀₂₇, it disappears. The conducted experimental studies show a number of conclusions of utilitarian importance. The highest sensitivity to bending for the TFBBG structure ($\theta = 2^\circ$) can be achieved by measuring the spectral shifts of the lowest order modes, but it is not included in the ghost mode, *e.g.*, for the LP₀₆ mode. However, this mode is closest to the ghost type, and moving it causes its absorption by the ghost after exceeding a certain value of the bend radius. This causes both the limitation of the measuring range and the distortion of its spectral characteristics as it approaches the ghost mode. Figure 7 shows the wavelengths of individual modes for the initial state, *i.e.*, for the bend radius $R = 30$ mm and the final state corresponding to the bending radius of the fiber equal to $R = 15$ mm.

Figure 7a shows the changes in the wavelength of modes with the azimuth number $m = 0$, while Fig. 7b shows the modes with the number $m = 1$. As seen, the initial and final wavelengths differ only for modes up to a certain limit radial number n . The limit at which due to bending

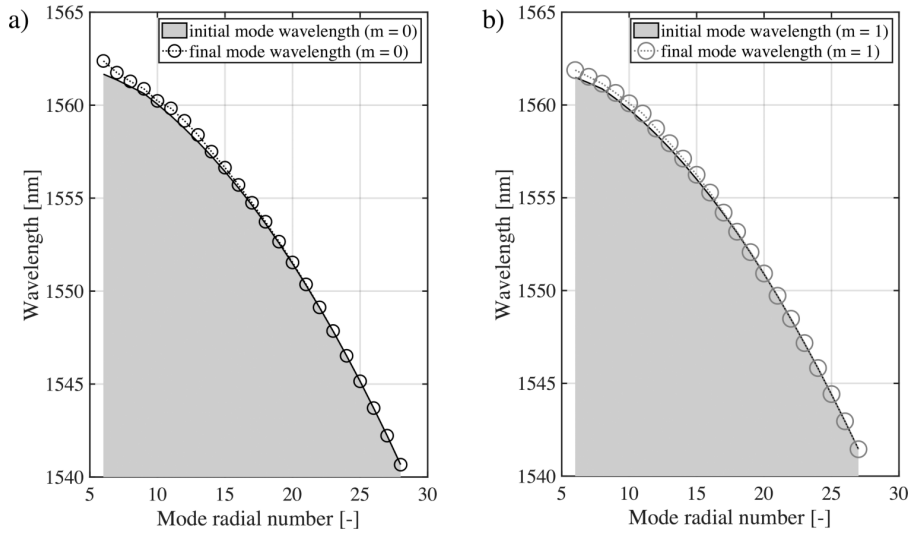


Fig. 7. Changes in wavelengths for modes with azimuth numbers $m = 0$ (a) and $m = 1$ (b).

there is no longer a wavelength shift, however, depends not only on the radial number of the mode but also on its azimuth number. For the group of modes with the number $m = 0$, the first mode for which there is no difference between the initial and the final wavelength is the mode with the radial number $n = 23$. In turn, for the modes for which $m = 1$, the first mode that does not experience a wavelength shift due to bending is the mode with $n = 26$.

Analyzing the measurement results presented in Fig. 8, it can be seen that from the point of view of maximizing the sensitivity to bending in the considered measuring range, it is most advantageous to measure the spectral shifts of the modes with the maximum values of the wavelength shift. Note that there are a few modes for which the value of such a shift is close to or greater than 400 nm. In particular, these are the LP_{16} , LP_{06} , LP_{17} , LP_{011} , LP_{111} and LP_{112} modes. In the case of a grating with the angle $\theta = 2^\circ$, this spectral range is the most sensitive to bending and simultaneously reacts within a wide range of changes in the bending radius.

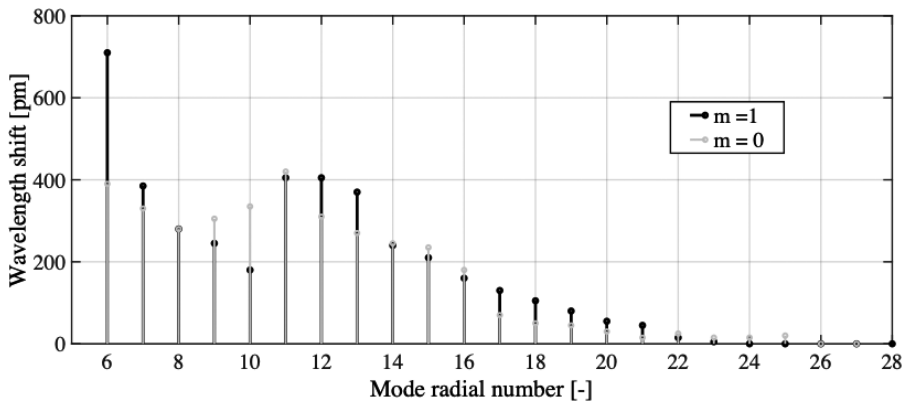


Fig. 8. Values of spectral shifts for all LP_{0n} and LP_{1n} modes due to TFBG bending in the x -axis.

3.2. Changes in the shape of the spectral characteristics of TFBG optical fibers

Apart from changing the wavelength of TFBG cladding modes, there is another phenomenon related to the bending of TFBG optical fibers. It consists of changing the shape of individual minima derived from specific cladding modes. To discuss both of these phenomena, the figures below show the changes in the spectra of individual modes following the induced TFBG bending. There is such a spectral range in which the spectral characteristics of the cladding mode take the form of one minimum experience split into two distinct minima. The phenomenon of peak splitting on the spectral characteristics, derived from the cladding modes, occurs most strongly in the spectral range from 1556 nm to 1559 nm, as shown in Fig. 9. This spectral range includes modes with radial numbers with values between 13 and 15.

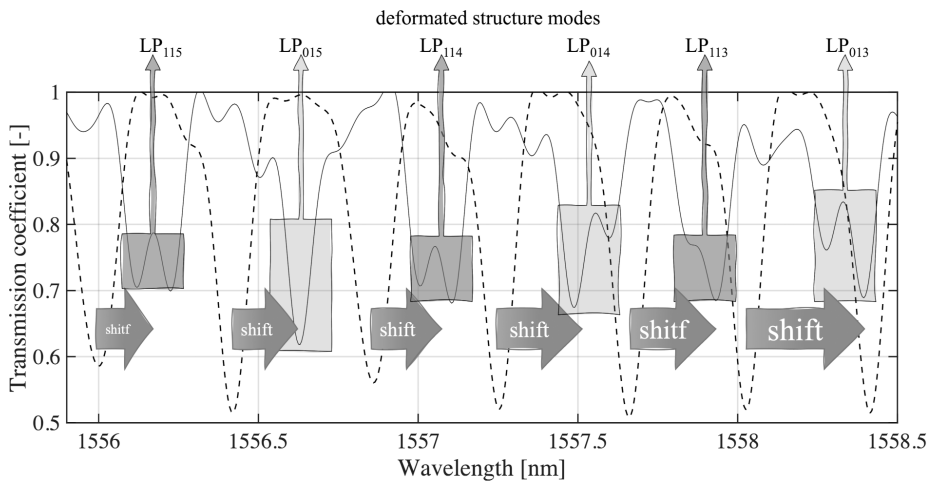


Fig. 9. Deformation and shift of minima related to the existence of modes with radial numbers 13–15. The dashed line shows the modes before the bending deformation, and the solid line shows the modes after the deformation.

The measurement results presented in Fig. 9 show a very interesting phenomenon consisting of the appearance of a second minimum corresponding to a given coat mode. In this study, this phenomenon is called the splitting of the minima derived from the cladding modes. The splitting of every second mode occurs in a much wider spectral range. However, the ever-weaker bending response of the lower order modes and the ever-smaller minimum heights make the spectral split more difficult to see. For the spectral range between 1540 nm and 1550 nm, the splitting is practically invisible, as is the spectral shift.

4. Discussion

The phenomena observed during the measurements can be explained by analyzing the propagation of the electromagnetic wave through the TFBG structure. These phenomena include spectral shift, peak shape change, peak broadening and cleavage. The response of the TFBG device to the bending of the optical fiber was explained in [15] and is related to the change in the effective tilt angle of the sensor. This explanation is not entirely complete because, in fact, the diameter of the optical fiber cladding is very small compared to the bending radius, which is usually a dozen or so centimeters. A bending radius of 15 cm creates a fiber loop with a circumference

of 94 mm, which is a value several orders larger with a cladding diameter of 150 mm. Due to the above, the effect of changing the angle of tilt of the TFGB planes described in [15] is so small that it can be ignored. In fact, the coupling coefficient of the individual cladding modes changes. This is in turn caused by the symmetry changes of the modes themselves. This conclusion comes from papers discussing the application of the coupled mode theory to calculate the energy carried by these particular modes in anisotropic optical fibers. It was shown in [19] that the modes of optical fibers are subjected to a bending shift outside the waveguide. On the other hand, when analyzing the results presented in [20], it can be noticed that the effective refractive indices of the sheath and core modes also change. Bending the TFGB fiber causes a relative elongation ε along this fiber. This is parallel to the optical axis of the fiber. Assuming that the fiber is bent in one plane with radius R and the bending force is parallel to the y -axis, we can write that the relative elongation will be given by the following equation:

$$\varepsilon = \frac{y}{R}. \quad (2)$$

In turn, the appearance of such an elongation along the optical fiber will change the refractive index in accordance with the photoelastic effect [21]. This change can be described with the equation below:

$$\Delta n = \frac{yn^3((1-\nu)p_{12} - \nu p_{11})}{2R}, \quad (3)$$

where ν is the Poisson ratio, p_{12} and p_{11} are photoelastic constants, and n is the refractive index. The Poisson constant is $\nu = 0.16$, while p_{12} and p_{11} are 0.252 and 0.113, respectively.

By analyzing (3), it can be concluded that the change in the refractive index due to bending of the optical fiber depends on the position along the y -axis. The value of Δn is equal to 0 in the fiber core exactly along its axis ($y = 0$). It can also be concluded that for the positive and negative positions on the y -axis, the change in refractive index Δn due to bending of the fiber has different signs. The lower part of the fiber, for which y is positive, is compressed by the bending, while the upper part, for which y is negative, is in tension. Only the layer located exactly in the middle of the fiber is neutral, *i.e.*, it is neither compressed nor stretched due to the bending of the structure. Note that according to (3), in the case of no bend, *i.e.*, for the bend radius reaching infinity Δn , it does not depend on the position along the y -axis because the more we bend an optical fiber, the greater changes in n we obtain. At the border of the cladding and the bending radius $R = 30$ mm, the absolute change in the refractive index will be $\Delta n = 1.25 \cdot 10^{-3}$, while in the case of bending with the radius $R = 15$ mm, the change in the refractive index is already more than 2 times greater and amounts to even $2.8 \cdot 10^{-3}$. The dependences above have a key impact on the shape changes and shifts of the spectral characteristics of the individual sheath modes of the TFGB structure subjected to bending. The appearance of a disturbance in the form of a diagonal Bragg grating in a single-mode fiber causes the light introduced into the optical fiber and propagating in the core to be coupled to a series of cladding modes. These modes have a strictly defined power distribution, which means that the intensity of the light propagating in individual modes is also strictly defined. They can be determined by numerically solving the equation of eigenvalues for LP modes [22].

As the azimuth number increases, so does the number of maxima on the light intensity distribution characteristics. When the radial number is equal to 1, there is one maximum for the azimuth number equal to 0. The modes with the same radial number but an azimuth number equal to 1 already have two maxima, while the modes for which $n = 1$ and $m = 2$ have 4 maxima. This known property of LP modes influences the behavior of the spectral characteristics of individual cladding modes propagating through the TFGB fibers.

According to (3), the lower part of the fiber for which y is negative is compressed by bending, while the upper part for which y is positive is in tension. Only the layer lying exactly in the middle of the fiber is neither compressed nor stretched due to the bending of the structure. For this reason, the LP_{01} mode is characterized by the lowest dependence of its power distribution on the bending radius of the fiber with TFBG. The diameter of the fiber core is much smaller than that of its cladding. To notice the change in the light power distribution, only those modes that are characterized by the greatest dependence of this profile on the structure's bending radius should be selected. These are mainly low-order modes for which a relatively large part of the light propagates at the interface between the cladding and the core and not only in the central part of the core. We also know that, according to the coupled-mode theory, the coefficient of light coupling to the cladding mode is partially dependent on the size of the surface inside the fiber core, in which the transverse distribution of the radiation intensity of the core mode and the input cladding mode coincide [23]. The LP_{0n} modes have the strongest local light intensity maxima in the fiber core near its longitudinal axis. This results in a strong overlap of their distribution with the intensity distribution of the input core mode LP_{01} . The LP_{1n} modes have a lower intensity in the central part of the fiber in its core, and therefore, the overlap of their distributions with the LP_{01} mode is smaller than in the case of the modes with the azimuth number $m = 0$.

5. Conclusions

This paper explains the physical phenomena leading to the shape change and spectral shift of the modes generated on the TFBG structure. The conditions under which the greatest spectral shifts can be obtained have been shown. It has also been shown that for a specific tilt angle of the diffractive planes of oblique Bragg structures, the selection of specific LP modes enables the selection of the maximum spectral shift when measuring fiber bend. The phenomena of distortion of the spectral characteristics of TFBG structures in the form of splitting of transmission minima originating from linearly polarized modes are presented, and the reasons for such deformations are explained. Modes whose measurement of spectral shifts is the most favorable from the point of view of maximizing the sensitivity to bending have also been indicated. In the future, the author intends to present and explain the phenomena of overlapping of individual minima resulting from specific fiber cladding modes and the utilitarian conclusions resulting from these phenomena, allowing for a more effective use of this type of transducer as bending sensors, both for optical fibers and other structural elements for which such fibers are assembled. The most important contribution of this work to the area of research on the use of TFBG structures as bending transducers is the analysis of spectral shifts and changes in the shape of spectral minima derived from modes with azimuthal numbers of 0 and 1 with similar radial numbers. Therefore, we can select spectral modes and ranges that allow us to extend the measurement range and reduce unnecessary distortion of spectral characteristics caused by the optical fiber bend. Manufacturing the structure with an angle of 2° and selecting the spectral range corresponding to the tenth linearly polarized mode with azimuth number 1 (LP_{110}) or the fifteenth mode with azimuth number 0 (LP_{015}) is most advantageous for the measurements using TFBG elements as bending transducers.

Acknowledgements

This work was supported by the Science Discipline Fund of Lublin University of Technology (grant # FD-EE-309).

References

- [1] Świrniak, G., & Mrocza, J. (2016). Approximate solution for optical measurement of the diameter and refractive index of a small and transparent fiber. *Journal of the Optical Society of America A, Optics, Image Science, and Vision*, 33(4), 667–676. <https://doi.org/10.1364/JOSAA.33.000667>
- [2] Onofri, F. R. A., Krzysiek, M. A., Barbosa, S., Messager, V., Ren, K.-F., & Mrocza, J. (2011). Near-critical-angle scattering for the characterization of clouds of bubbles: Particular effect. *Applied Optics*, 50(30), 5759–5769. <https://doi.org/10.1364/AO.50.005759>
- [3] Onofri, F., Krzysiek, M., & Mrocza, J. (2007). Critical angle refractometry and sizing of bubble clouds. *Optics Letters*, 32(14), 2070–2072. <https://doi.org/10.1364/OL.32.002070>
- [4] Tolegenova, A., Kisała, P., Zhetpisbayeva, A., Mamyrbayev, O., & Medetov, B. (2019). Experimental determination of the characteristics of a transmission spectrum of tilted fiber Bragg gratings. *Metrology and Measurement Systems*, 26(3), 581–589. <https://doi.org/10.24425/mms.2019.129585>
- [5] Ciężczyk, S., Kisała, P., Skorupski, K., Panas, P., & Klimek, J. (2018). Rotation and twist measurement using tilted fibre Bragg gratings. *Metrology and Measurement Systems*, 25(3), 429–440. <https://doi.org/10.24425/123893>
- [6] Harasim, D., Kisała, P., Yeraliyeva, B., & Mrocza, J. (2021). Design and Manufacturing Optoelectronic Sensors for the Measurement of Refractive Index Changes under Unknown Polarization State. *Sensors*, 21(21), 1–29. <https://doi.org/10.3390/s21217318>
- [7] Jin, L., Wang, Z., Fang, Q., Liu, Y., Liu, B., Kai, G., & Dong X. (2007). Spectral characteristics and bend response of Bragg gratings inscribed in all-solid bandgap fibers. *Optics Express*, 15(23), 15555–15565. <https://doi.org/10.1364/OE.15.015555>
- [8] Swanson, A. J., Raymond, S. G., Janssens, S., Breukers, R. D., Bhuiyan, M. D. H., Lovell-Smith, J. W., & Waterland, M. R. (2016). Development of novel polymer coating for FBG based relative humidity sensing. *Sensors and Actuators A*, 249, 217–224. <https://doi.org/10.1016/j.sna.2016.08.034>
- [9] Kisała, P., Harasim, D., & Mrocza J. (2016). Temperature-insensitive simultaneous rotation and displacement (bending) sensor based on tilted fiber Bragg grating. *Optics Express*, 24(26), 29922–29929. <https://doi.org/10.1364/OE.24.029922>
- [10] Kisała, P., Mrocza, J., Ciężczyk, S., Skorupski, K., & Panas, P. (2018). Twisted tilted fiber Bragg gratings: new structures and polarization properties. *Optics Letters*, 43(18), 4445–4448. <https://doi.org/10.1364/OL.43.004445>
- [11] Shao, L. Y., & Albert, J. (2010). Compact fiber-optic vector inclinometer. *Optics Letters*, 35(7), 1034–1036. <https://doi.org/10.1364/OL.35.001034>
- [12] Jin, Y. X., Chan, C. C., Dong, X. Y., & Zhang, Y. F. (2009). Temperature-independent bending sensor with tilted fiber Bragg grating interacting with multimode fiber. *Optics Communications*, 282(19), 3905–3907. <https://doi.org/10.1016/j.optcom.2009.06.058>
- [13] Dong, X., Liu, Y., Shao, L. Y., Kang, J., & Zhao, Ch. L. (2011). Temperature-Independent Fiber Bending Sensor Based on a Superimposed Grating. *IEEE Sensors Journal*, 11(11), 3019–3022. <https://doi.org/10.1109/JSEN.2011.2157124>
- [14] Amanzadeh, M., Aminossadati, S. M., Kizil, M. S., & Rakić, A. D. (2018). *Measurement*, 128, 119–137. <https://doi.org/10.1016/j.measurement.2018.06.034>
- [15] Baek, S., Jeong, Y., & Lee B. (2002). Characteristics of short-period blazed fiber Bragg gratings for use as macrobending sensors. *Applied Optics*, 41(4), 631–636. <https://doi.org/10.1364/AO.41.000631>

- [16] Liu, B., Miao, Y., Zhou, H., & Zhao Q. (2008). Research on Pure Bending characteristic of tilted fiber Bragg grating. *IEEE Optical Fiber Sensors Conference*, 1–4. <https://doi.org/10.1109/APOS.2008.5226323>
- [17] Guo, T., Chen, Ch., Laronche, A., & Albert, J. (2008). Power-Referenced and Temperature-Calibrated Optical Fiber Refractometer. *IEEE Photonics Technology Letters*, 20(8), 635–637. <https://doi.org/10.1109/LPT.2008.919457>
- [18] Erps, J. V., Debaes, C., Nasilowski, T., Mergo, P., Wojcik, J., Aerts, T., Terryn, H., Watté, J., & Thienpont, H. (2008). A low loss 180 degrees coupling fiber socket making use of low bending loss hole-assisted fiber. *Proc. SPIE 6992*, 1–8. <https://doi.org/10.1117/12.778649>
- [19] Marcuse, D., (1973). Coupled mode theory of round optical fibers. *The Bell System Technical Journal*, 52(6), 817–842. <https://doi.org/10.1002/j.1538-7305.1973.tb01992.x>
- [20] Block, U. L., Dignonnet, M. J. F., Fejer, M. M., & Dangui, V. (2006). Bending-induced birefringence of optical fiber cladding modes. *Journal of Lightwave Technology*, 24(6), 2336–2339. <https://doi.org/10.1109/JLT.2006.874566>
- [21] Marcuse, D. (1976). Field deformation and loss caused by curvature of optical fibers. *Journal of the Optical Society of America*, 66(4), 311–320. <https://doi.org/10.1364/JOSA.66.000311>
- [22] Silva, R. M., Ferreira, M. S., & Frazão, O. (2012). Temperature independent torsion sensor using a high-birefringent Sagnac loop interferometer. *Optics Communications*, 285, 1167–1170. <https://doi.org/10.1016/j.optcom.2011.11.119>
- [23] Erdogan, T., & Sipe J. (1996). Tilted fiber phase gratings. *Journal of the Optical Society of America A*, 13(2), 296–313. <https://doi.org/10.1364/JOSAA.13.00029>



Piotr Kisala received from M.Sc. diploma in informatics and computer networks from Maria Curie-Skłodowska University, Poland. He received a Ph.D. degree in 2009, a habilitation degree in 2013 and the title of professor in 2020. He is currently head of the Optoelectronic & ICT Department at Lublin University of Technology. His research interests include optical sensor projects, fabrication and testing and the design and development of unconventional FBG sensors. Prof.

Kisala has authored over 80 journal publications and conference contributions and 6 patents.